



Conference of Fundamental Research and Particle Physics, 18-20 February 2015, Moscow, Russian Federation

Optimization of the neutron detector design based on the ${}^6\text{LiF}/\text{ZnS}(\text{Ag})$ scintillation screens for the GAMMA-400 space observatory

I.I. Gnezdilov*, G.L. Dedenko, R.F. Ibragimov, V.A. Idalov, V.V. Kadilin, A.A. Kaplun, A.V. Klemetiev, V.I. Mukhin, A.A. Taraskin, E.M. Turin, R.N. Zaripov

National Research Nuclear University MEPhI (Moscow Engineering Physics Institute), Kashirskoe Shosse 31, Moscow 115409, Russia

Abstract

The Neutron Detector (ND) is a new detector sub-system for the future GAMMA-400 space observatory. It aims to complement the instrument's GAMMA-400 electromagnetic calorimeter (CsI(Tl), total depth is $25.0 X_0$) in identifying cosmic-ray electrons from ~ 100 MeV up to 3 TeV. Such electrons are of significant scientific interest, but their identification is complicated by the overwhelmingly more abundant hadronic cosmic rays, hence making significant hadronic rejection power of paramount importance. Particle showers initiated by nuclei in the GAMMA-400 calorimeter have a profile different from an electron-induced electromagnetic cascade, and the hadron rejection power deriving from this difference can be significantly enhanced by making use of the thermal neutron activity at late (>100 ns) times relative to the start of the shower. Indeed hadron-induced showers tend to be accompanied by significantly more neutron activity than electromagnetic showers. In the described ND for capturing thermalized neutrons applied isotope ${}^6\text{Li}$, which is part of the scintillation screen ${}^6\text{LiF}/\text{ZnS}(\text{Ag})$. ND placed are under the electromagnetic calorimeter. The results GEANT4 simulation of the ND shows that ND has high neutron detection efficiency. © 2015 The Authors. Published by Elsevier B.V. This is an open access article under the CC BY-NC-ND license (<http://creativecommons.org/licenses/by-nc-nd/4.0/>).

Peer-review under responsibility of the National Research Nuclear University MEPhI (Moscow Engineering Physics Institute)

Keywords: calorimeter; electron; GAMMA-400; gamma-ray; hadron; ${}^6\text{LiF}/\text{ZnS}(\text{Ag})$; neutron detector; observatory; orbital; rejection; shower

1. Introduction

In many physics experiments where calorimeters are employed, the requirement of an accurate energy

* Corresponding author. Tel.: +7-495-788-5699.

E-mail address: y.gnezdilov@gmail.com

measurement is accompanied by the requirement of very high hadron-electron rejection power. Normally the latter requirement is achieved by designing a high-granularity detector with sufficient depth so that the showers can fully develop. This method has many drawbacks ranging from the high number of electronic channels to the high mass of the detector itself. Some of these drawbacks may in fact severely limit the deployment of such a detector in many experiments, most notably in space-based ones. Another method based on the measurement of the number of neutrons outgoing from the calorimeter, was first used in the orbital spectrometer PAMELA [1]. Two devices of the PAMELA spectrometer were used in the experiment: the calorimeter and the ND. The calorimeter is composed of layers of tungsten absorber and silicon detectors planes. The total depth is about 16.3 radiation lengths and about 0.6 interaction length. The ND is placed under the calorimeter. The size of the ND is $60 \times 55 \times 15 \text{ cm}^3$. It contains 36 ^3He -counters surrounded by the polyethylene moderator $\sim 9 \text{ cm}$ thick. However, ^3He -counters has low neutron registration efficiency due to their slow response: time resolution in proportional mode is $\sim 2 \mu\text{s}$. When a high-energy hadron interacts inside the calorimeter, a large number of neutrons from the decay of excited nucleus are produced, while if a primary particle is a lepton the number of neutrons generated in the photonuclear interactions, mainly from the giant resonance, is 10–20 times lower. A part of these neutrons is thermalized by the polyethylene moderator and detected by the ^3He -counters. The implementation of the ND increases a rejection factor of hadrons from electrons with energies of 20–180 GeV about ten times.

The GAMMA-400 space observatory has been designed for the optimal detection of gamma-rays in a broad energy range (from $\sim 100 \text{ MeV}$ up to 3 TeV), with excellent angular and energy resolution. The observatory will also allow precise and high statistic studies of the electron component in the cosmic rays up to the multi TeV region, as well as protons and nuclei spectra up to the knee region. The GAMMA-400 space observatory will allow to address a broad range of science topics, like search for signatures of dark matter, studies of Galactic and extragalactic gamma-ray sources, Galactic and extragalactic diffuse emission, gamma-ray bursts and charged cosmic rays acceleration and diffusion mechanism up to the knee. The instrument contains two calorimeters CC1 and CC2 based on CsI(Tl) total depth is about $25.0 X_0$ or $1.2 \lambda_0$ (λ_0 is nuclear interaction length) [2]. The ND is placed under the calorimeter. The size of the ND is $100 \times 100 \times 10 \text{ cm}^3$. The ND contribution in the rejection factor for protons in the GAMMA-400 space observatory is considered with significantly different number of neutrons generated in the electromagnetic and hadronic cascades. In cascades, induced by protons, the generation of neutrons is more intensive than in the electromagnetic shower. The source of neutrons in cascades, induced by electrons, concerns mainly with generation of gamma-rays in those cascades with energy close to 17 MeV. These gamma-rays, in turn, could generate neutrons in the GEANT4 resonance reaction. Analyzing information from the ND placed just under the

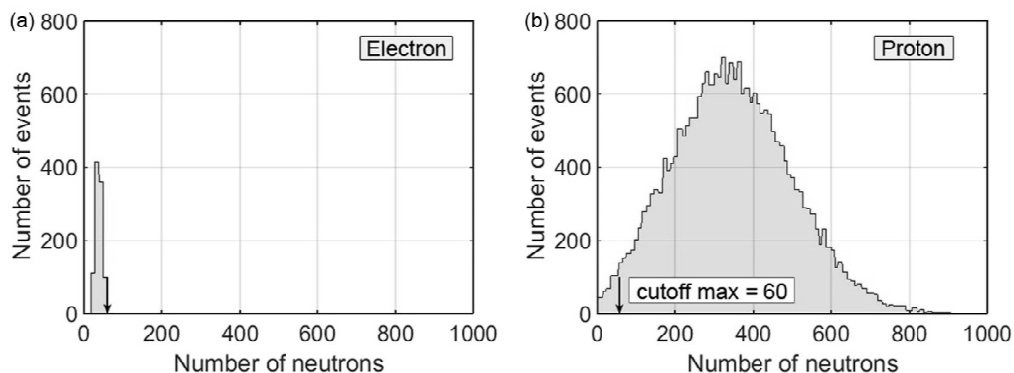


Fig. 1. The distributions of number of neutrons at the entrance of ND from initial (a) electrons with $E_e = 100 \text{ GeV}$ and (b) protons with $E_p \geq 250 \text{ GeV}$ (the proton energy spectral index is equal to -2.7) [3].

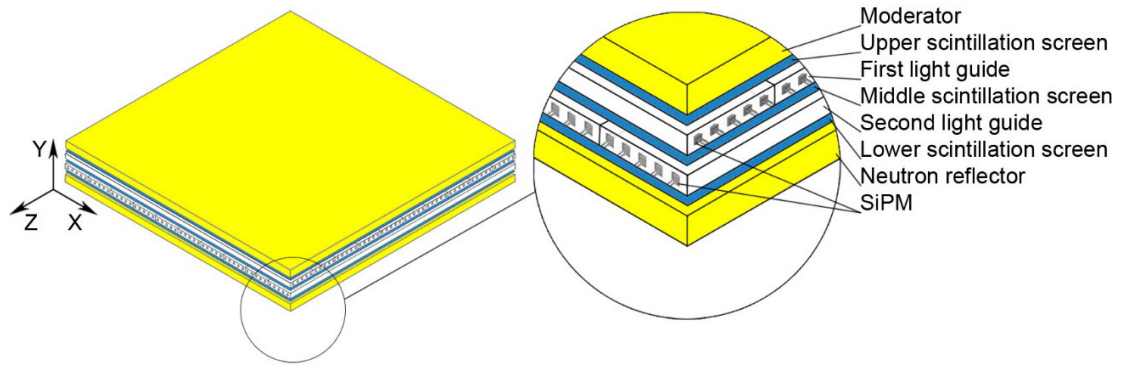


Fig. 2. Schematic drawing of the ND.

calorimeter, it is possible to suppress protons by the factor of 400. The distributions for number of neutrons at the entrance of ND from initial electrons and protons are shown in Fig. 1. The cutoff for the number of neutrons to separate protons is equal to 60[3]. The efficiency of ND is not taken into account in the present simulation.

The purpose of this work was the ND construction optimization to increase neutron detection efficiency.

2. The design of the ND for the GAMMA-400

As shown in Fig. 2, the ND for GAMMA-400 consists of successive layers of hydrogenous material and ${}^6\text{LiF}/\text{ZnS}(\text{Ag})$ scintillation screens (3 layers). It uses commercial scintillation screens, manufactured by Eljen Technology and Applied Scintillation Technologies (now known as Scintacor). Scintillation screens are optically contacts with two layers of the light guides which are made from polymethylmethacrylate (PMMA) in a $100 \times 10 \times 1.5 \text{ cm}^3$ size band form. There are 10 light intercepting bands in the each layer. By the scintillation the light is register 5 SiPM with sensing surface which size is $6 \times 6 \text{ mm}^2$, placed on the butt of each of the bands. In sum is used 200 SiPM, which are coupling per 5 pieces across to each other and makes 40 channels register, that gives an opportunity to increase flow intensity of the traceable neutrons.

The first and the second layers of the light guides locate mutual perpendicular. Such ply arrangement allows receive spatial registered neutrons distribution amount on the XZ plane on at the ND half-height. As implied by figure on the Fig. 3, given in the article[4], the spatial neutron distribution information may have additional application for the electron and proton showers rejection.

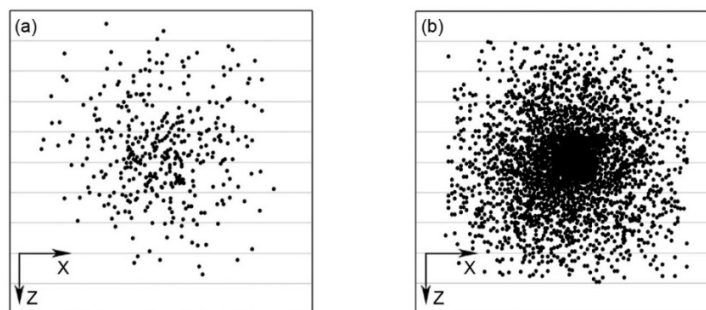


Fig. 3. The spatial registered neutrons distribution amount on the XZ plane on at the ND half-height during interaction in the calorimeter matter (a) with 400 GeV energy electron and (b) with 1000 GeV energy proton, obtained by a modeling of the GEANT4[4].

2.1. Moderator and neutron reflector

Moderator and neutron reflector layers are 3-cm and 4-cm thick respectively and both consist of high-density polyethylene. Optimal thicknesses were chosen by numerical simulation method, which is described in the section 3.

2.2. Scintillation screen

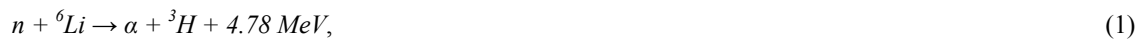
${}^6\text{LiF}/\text{ZnS}(\text{Ag})$ scintillation screens using in the ND construction for the GAMMA-400 was proposed in the article[5]. The $\text{ZnS}(\text{Ag})$ scintillator doped with ${}^6\text{LiF}$ is a thermal neutron convertor. The lithium is enriched in ${}^6\text{Li}$ to a minimum of 95 atom %. Scintillation screen consisting of a homogeneous matrix of fine particles ${}^6\text{LiF}$ and $\text{ZnS}(\text{Ag})$, compactly dispersed in a colorless binder.

Properties commercially scintillation screens are shown in the Table 1.

Table 1. Properties commercially scintillation screens.

№	Type scintillation screens	${}^6\text{LiF}:\text{ZnS}$ mix ration by weight	${}^6\text{Li}$ isotope estimated atomic volume density, atoms/ccx10 ²¹	Thickness, mm	Estimated thermal neutron capture efficiency, %
1	EJ-426-0	1:3	8.81	0.32	23
2	EJ-426-0	1:3	8.81	0.50	34
3	EJ-426HD2	1:2	13.9	0.32	34
4	EJ-426HD2	1:2	13.9	0.50	48
5	AST	1:4	7.77	0.25	17
6	AST	1:4	7.77	0.45	28
7	AST	1:2	12.9	0.25	26
8	AST	1:2	12.9	0.45	42

Neutrons are detected by the following neutron reaction:



with a cross section of 941 barns for 0.025 eV neutrons, where kinetic energy of the α particle is 2.05 MeV, the kinetic energy of ${}^3\text{H}$ particle is 2.73 MeV. The resulting triton and alpha particle are detected by $\text{ZnS}(\text{Ag})$ phosphor with the broad blue fluorescent spectrum with wavelength of maximum emission 450 nm shown on Fig.4(a) and Fig. 4(b) (black color dotted line). Each stopped thermal neutron will liberate 1.75×10^5 photons. The decay time of the prompt scintillation component is 0.2 μs .

2.3. Light guides and registration light

The ND applies using the 1.5-cm thick light guides $100 \times 10 \text{ cm}^2$ made from PMMA. The thickness of these guides was determined by the numerical simulation described in the section 3. The ND contains 20 light guides. At the ends of each light guide with $10 \times 1.5 \text{ cm}^2$ section ten SiPMs (SensL MicroFC-60035-SMT, sensor active area $6 \times 6 \text{ mm}^2$) were placed (400 SiPM total).

In considering the graphics in the Fig. 4a we can learn, that SiPMs are more effective compared to PMTs. There are ~ 1.6 times more photoelectrons produced when using SiPMs over PMTs, because of the higher quantum efficiency and better cross-section with the emitting spectrum of the scintillator $\text{ZnS}(\text{Ag})$. Wavelength shifting plastics (WLSP) can be effectively used as a light guide material.

The green-emitting WLSP, for example, EJ-280 is ideal for shifting the emission spectra of common blue scintillators. The most common use for green WLSP is in the form of long narrow bars air-coupled to blue scintillators arrayed either in flat planes or in stacks. The bars provide a compact means of light collection. The green light is effectively turned 90° as a result of the isotropic re-emission, and is transmitted by total internal

reflection to phototubes at both ends of the bar to achieve a highly uniform light collection. While there is a typical 75% loss of signal amplitude in these systems, they can provide advantages over conventional light collection methods. The quantum efficiency of the fluorescent dopant in EJ-280 is 0.86, and its decay time under laser excitation is 8.5 ns. The plots on the Fig. 4b confirms the WLSP using efficiency in the optical light guide for a light collecting scintillation ZnS(Ag). Optical light guide efficiency from WLSP increases light collecting[6]. Also, as can be seen from the Fig. 4c, SiPMs produce ~2.3 times more photoelectrons than PMTs.

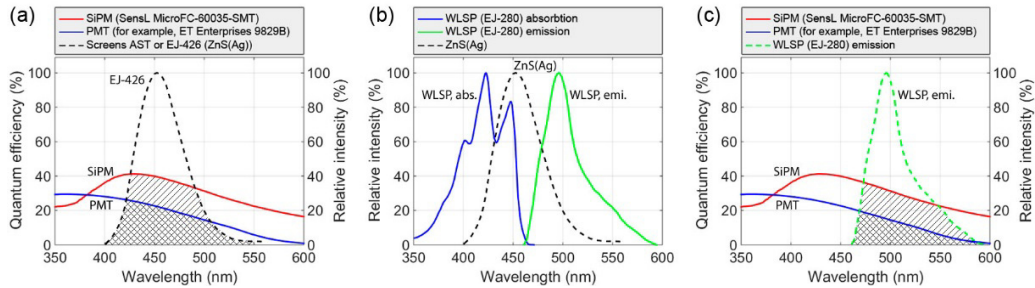


Fig. 4. (a) the emitting spectrum of the scintillator ZnS(Ag) and (b) spectral response curves of PMT & SiPM, and spectrum of the scintillator ZnS(Ag) and the absorbing & emitting spectra of the WLSP; (c) spectral response curves of PMT & SiPM and emitting spectra of WLSP.

3. GEANT4 simulation and results

GEANT4 software toolkit is used for simulation and the Monte Carlo calculations of the neutron absorption efficiency of ND. The detection efficiencies obtained would be dependent on the efficiency of optical coupling to the photosensor: SiPM or PMT. These detectors may be viewed directly with photosensors or indirectly by means of PMMA or green WLSP.

Neutron absorption efficiency (ϵ_a) is defined as the number of alpha-particles (N_α) that generates in the scintillation screens by reaction (1) divided by the number of neutron (N_n) outgoing calorimeter and cross ND:

$$\epsilon_a = N_\alpha / N_n, \tag{2}$$

Neutron detection efficiency (ϵ_d) is defined as:

$$\epsilon_d = N_{count\ observed} / N_n = (N_\alpha \times P) / N_n = \epsilon_a \times P, \tag{3}$$

where $N_{count\ observed}$ — number of counts observed by the ND divided by N_n , P is the probability of a scintillation flash caused by interaction between an alpha-particle and a scintillator multiplied by the probability of its detection by a photodetector. In the report [7] shows the experimental measuring absolute neutron detection efficiency results for Symetrica NNS:4000 radiation monitor. Like a ND, it contains the light guide and two ${}^6\text{LiF}/\text{ZnS}(\text{Ag})$ scintillation screens. On the basis of absolute neutron detection efficiency and received GEANT4 simulation ϵ_a comparison it was defined, that $P \approx 0.5$.

In the electromagnetic cascade neutrons result from photonuclear reactions of the secondary gamma-rays with nuclei of medium and the collapse of the nuclei at hadron interactions. In interactions of high-energy hadrons with nuclei of medium (especially with heavy nuclei), along with charged particles, there is produced a great quantity of neutrons. In considering the kinematics of such interactions, one can select in a first approximation three basic regions of production of particles. The first is connected with fragmentation of an incident nucleus with production of neutrons in a narrow forward cone along the beam with energies, that are close to the energy of a projectile particle that is reduced by one nucleon.

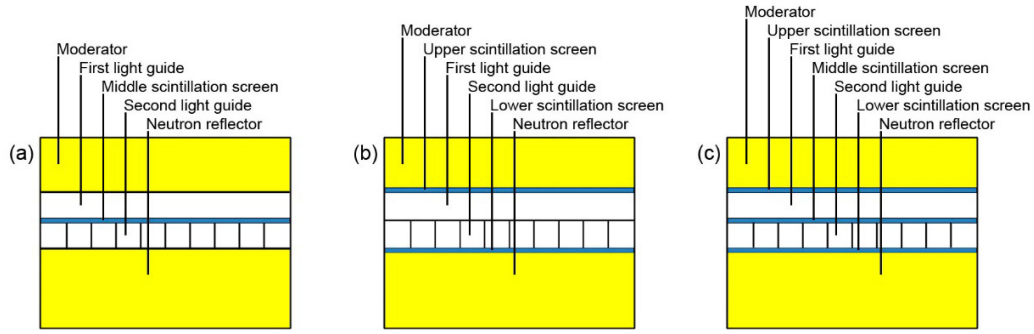


Fig. 5. Schematic drawing of the ND 100×100×10 cm³ that were used in the simulation:(a) one layer scintillation screen,(b) two layer scintillation screens, (c) three layer scintillation screens.

Here elastic and quasi-elastic interaction with charge-exchange of incident protons can be attributed. The second region, which forms a hard neutron spectrum at large angles, is a region of intersection of colliding nuclei that is a zone of interaction of nucleon participants of collision. Decay of the residual nucleus of a target gives a low-energy evaporative neutron emission and presents the third region of neutron production. The average energy of evaporated neutrons is ~ 2 MeV, they have an isotropic angular distribution. GEANT4 simulations shows that an energy spectrum of outgoing neutrons contains about 60% neutrons with energy < 1 MeV for 1 TeV initial proton energy, while this value reaches 90% for 400 GeV initial electrons. Thus it could be assumed, that an energy spectrum of outgoing neutrons could be simulated by ²⁵²Cf source spectrum with average neutron energy of ~ 2.2 MeV. The number of incident neutrons was 10⁶ neutrons.

In all cases plane-parallel flux of neutrons is incident to the ND, which schemes are shown in the Fig. 5.

As shown in the Fig. 6a, neutron absorption efficiency ND which encloses scintillation screen with atomic volume density ⁶Li or 7.77×10²¹ at/cm³ to 13.9×10²¹ at/cm³ increases only within 6% range. Thus, it is possible to use any kind of commercial screens (listed in table 1) for the ND construction. The maximum of the ND neutron absorption efficiency can be achieved using three layers of scintillation screens.

Fig. 6b shows that neutron absorption efficiency of a three-layered detector increases significantly within overall light guide thickness range from 1 to 3-cm. Thus, 1.5-cm thick light guide layer is considered optimal for the ND for GAMMA-400.

The calculated error in determining the neutron absorption efficiency on Fig. 6a and Fig. 6b is about 1%.

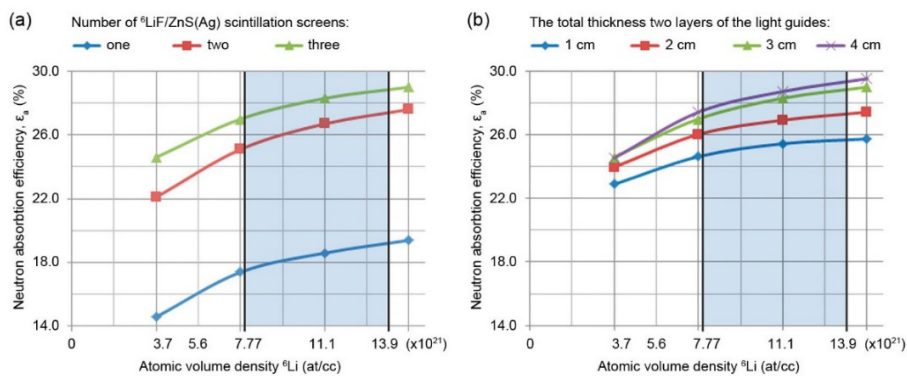


Fig. 6. Neutron absorption efficiency as function of ⁶Li atomic volume density for modeled ND: (a) with one up to three scintillation screens, (b) with three scintillation screens and two layers of the light guides, the latter of which have overall thickness from 1-cm to 4-cm.

Thus, the neutron absorption efficiency for the ND for GAMMA-400 equals to $\sim 28\%$ for atomic volume densities of ${}^6\text{Li}$ in range from 7.77×10^{21} at/cc to 13.9×10^{21} at/cc. Neutron detection efficiency for ${}^{252}\text{Cf}$ spectrum equals to $\sim 13\%$ on the assumption that the density of flux of neutrons is low and the ND registers outgoing neutrons not counting losses and light guides made of PMMA. ND operation speed impact research on the neutron detection efficiency will be further subject of research.

4. Conclusions

The ND using commercial ${}^6\text{LiF}/\text{ZnS}(\text{Ag})$ scintillation screens has been proposed for purposes of e/h rejection during orbital space measurements. Rejection principle is based on a number of detected moderated neutrons produced in a calorimeter. This number differs for different types of primary particles (electrons, positrons or protons). Second, auxiliary method of rejection is based on a spatial distribution of events in the detector plane. The ND is predominantly made from polyethylene, it has sizes of $100 \times 100 \times 10 \text{ cm}^3$ and weight of 110 kg, overall square of scintillation screens equals to 3 m^2 . The detector uses 200 SiPMs (sensor active area $6 \times 6 \text{ mm}^2$). The ND was designed to be used as part of the GAMMA-400 space observatory.

Acknowledgements

The authors acknowledges our colleagues Aleksey Leonov and Yury Trofimov for the helpful discussions on e/h rejection and cosmic X-ray background.

References

- [1] Stozhkov Y.I., Basili A., Bencardino R. et al. About separation of hadron and electromagnetic cascades in the PAMELA calorimeter. *International Journal of Modern Physics A* 2005;20(29):6745–6748.
- [2] Galper A.M., Adriani O., Aptekar R.L. et al. Characteristics of the GAMMA400 Gamma-Ray Telescope for Searching for Dark Matter Signatures. *Bulletin of the Russian Academy of Sciences. Physics* 2013;77(11):1339–1342.
- [3] Leonov A.A., Galper A.M., Bonvicini V. et al. A separation of electrons and protons in the GAMMA-400 gamma-ray telescope. arXiv:1503.06657v1 [astro-ph.IM] 2015.
- [4] Thant Zin, Kadilin V.V., Dedenko G.L. The estimation of the time and space response of the neutron detector in the composition of GAMMA-400 telescope. *Natural and Technical Sciences* 2012;6:37–40.
- [5] Mukhin V.I. Polycrystalline scintillator neutron detector. 3d International Conference on Engineering of Scintillation Materials and Radiation Technology ISMART-2012, Dubna, 2012;59–60.
- [6] Ely J.H., Bliss M., Kouzes R.T. et al. Final Technical Report for the Neutron Detection without Helium-3 Project. PNNL-23011 2013.
- [7] McClure J.C. A Report on the Observed Performance of the Symetrica Neutron Detection System for use in Radiation Portal Monitors. Report number 59620. Radiation Metrology Group, Health Protection Agency; 2010.